Two interacting electrons in a three-dimensional parabolic quantum dot: a simple solution

1998 J. Phys.: Condens. Matter 10 7857

(http://iopscience.iop.org/0953-8984/10/35/018)

J. Phys.: Condens. Matter **10** (1998) 7857–7867. Printed in the UK PII: S0953-8984(98)92197-X

Two interacting electrons in a three-dimensional parabolic quantum dot: a simple solution

G Lamouche and G Fishman

Laboratoire de Spectrométrie Physique, UMR C5588, Université Joseph Fourier, Grenoble 1, CNRS BP 87, 38402 St Martin d'Hères Cédex, France

Received 3 March 1998, in final form 9 June 1998

Abstract. We present a simple solution to the problem of two interacting electrons confined by a three-dimensional parabolic potential. The method relies on the diagonalization of the Hamiltonian in reduced Hilbert space. The basis functions are the solutions of the centre-of-mass motion and the relative motion of the two particles without Coulomb interaction. Since the Coulomb interaction only affects the relative motion, the matrix elements of the Hamiltonian are easily evaluated analytically. The numerical diagonalization is readily performed as only a few basis functions are needed to obtain a good precision on the energy levels: six basis functions ensure a precision better than 0.1% on the ground-state energy, while three basis functions are enough to obtain a precision better than 1%. The results are analysed and compared to previously published results. They are also used to evaluate the precision of a first-order perturbation calculation for the Coulomb interaction and an approach based on a $1/r^2$ approximate interaction potential for which there exists an analytical solution.

1. Introduction

In the last few years, there has been an increasing interest in the problem of quantum dots containing a few electrons [1]. These few-body systems are very attractive since they show properties that are strongly dependent on the number of electrons. They form the basis of low-consumption and fast electronic and optoelectronic devices. We cite for example the recent interest in single-electron-memory devices [2–4].

Most of the experimental and theoretical investigations in this field have focused on quantum dots made out of laterally confined two-dimensional electronic gases. With the rapid evolution of fabrication techniques, the interest in other types of quantum dots should grow in the near future. The experimental investigations have allowed the characterization of the energy level structure of a quantum dot [5–7]. Interesting phenomena like singlet–triplet transitions have been observed on systems containing as few as two electrons [5].

From a theoretical point of view, these few-body systems represent a challenging problem. The standard tools of the condensed-matter physicist like the many-body techniques relying on Hartree or Hartree–Fock approximations are often not sufficient since the exchange and correlation energies can be far from negligible [8]. A fully quantum mechanical treatment is needed. In the general case, this requires numerical calculations that can become quite time-consuming as the number of electrons grow.

There are, however, a few problems that can be solved easily. One is the problem of two interacting electrons confined in a quantum dot defined by a three-dimensional parabolic potential. This is a next-to-trivial problem. A two-electron system is obviously the minimal

0953-8984/98/357857+11$19.50

system for studying particle interaction. The parabolic potential can be considered as a zeroth-order approximation of any isotropic confining potential. This simple problem is nevertheless very useful since it allows the evaluation of the order of magnitude of many parameters as a function of the localization of the electrons. Additionally, the solutions can serve as a reference for estimating various approximation schemes or as a test case for more elaborate numerical treatments.

The problem of two interacting electrons in a three-dimensional parabolic potential has previously been studied by Zhu *et al* [9]. Their treatment is based on asymptotic series evaluated for both large and short distances between the interacting particles. The problem is solved by connecting those asymptotic expressions using a matching process described in [9]. Their results show interesting features such as crossing of levels as the strength of the parabolic potential is varied.

In the present paper, we offer an alternative solution to this problem. Our method relies on the standard diagonalization of the Hamiltonian in a reduced Hilbert space, using the eigenstates of the system without Coulomb interaction as a basis. Since only the relative motion of the electrons is affected by the Coulomb repulsion, the matrix elements are easily evaluated analytically. Only a few basis functions are needed to achieve a good precision, so the numerical diagonalization is readily performed. Our method leads to the solution in a much simpler manner than the method of [9]. Additionally, our resulting eigenfunctions are given by a single expression valid over all space while the method of [9] leads to various expressions, depending on the distance between the electrons.

In section 2, we present the theoretical framework underlying our approach. In section 3, the eigenstates are determined for various degrees of confinement. The energy levels are discussed and compared to previously published results. The variation of the wavefunctions with the strength of the quantum-dot potential is illustrated. The results are also used to evaluate the precision of two approximation methods: a first-order perturbation calculation for the Coulomb interaction and an approach based on an approximate $1/r^2$ potential for which there is an analytical solution. The main results are summarized in section 4.

2. Theoretical framework

The time-independent Schrödinger equation describing two interacting electrons of effective mass m^* in a quantum dot defined by a three-dimensional parabolic potential of frequency ω is

$$\underbrace{\left[-\frac{\hbar^2}{2m^*}\nabla_1^2+\frac{1}{2}m^*\omega^2 r_1^2-\frac{\hbar^2}{2m^*}\nabla_2^2+\frac{1}{2}m^*\omega^2 r_2^2+\frac{e^2}{4\pi\epsilon|\boldsymbol{r}_1-\boldsymbol{r}_2|}\right]}_{H}\Psi_{NLM,nlm}(\boldsymbol{r}_1,\boldsymbol{r}_2)$$
$$=E_{NL,nl}\Psi_{NLM,nlm}(\boldsymbol{r}_1,\boldsymbol{r}_2) \tag{1}$$

where ϵ is the static dielectric permittivity of the medium. The meaning of the various indices are clarified in the following. There are two lengthscales that are related to the problem and that will be used later: the oscillator characteristic length $l_0=[\hbar/(m^*\omega)]^{1/2}$ and the effective Bohr radius for an hydrogenic donor impurity $a_0^*=4\pi\epsilon\hbar^2/(m^*e^2)$.

It is quite straightforward to separate this problem in a centre-of-mass motion and a relative motion characterized by the coordinates $\boldsymbol{R}=(\boldsymbol{r}_1+\boldsymbol{r}_2)/2$ and $\boldsymbol{r}=\boldsymbol{r}_1-\boldsymbol{r}_2$,

respectively. The resulting Schrödinger equations are

$$\underbrace{\left[-\frac{\hbar^2}{2(2m^*)}\nabla_{\boldsymbol{R}}^2+\frac{1}{2}(2m^*)\omega^2R^2\right]}_{H^{CM}}\Phi_{NLM}(\boldsymbol{R})=E_{NL}\Phi_{NLM}(\boldsymbol{R}) \tag{2}$$

and

$$\underbrace{\left[-\frac{\hbar^2}{2(m^*/2)}\nabla_{r}^2+\frac{1}{2}\left(\frac{m^*}{2}\right)\omega^2r^2+\frac{e^2}{4\pi\epsilon r}\right]}_{H^{rel}}\phi_{nlm}(\boldsymbol{r})=E_{nl}\phi_{nlm}(\boldsymbol{r}). \tag{3}$$

Let us first consider the centre-of-mass motion. Equation (2) is the Schrödinger equation for a three-dimensional harmonic oscillator with a particle of mass $2m^*$. It is a textbook problem to find its solutions in spherical coordinates [10, 11]. The eigenenergies are given by

$$E_{NL}=\left(2N+L+\frac{3}{2}\right)\hbar\omega \tag{4}$$

while the eigenfunctions are given by

$$\Phi_{NLM}(\boldsymbol{R})=\frac{2^{3/4}}{l_0^{3/2}}Y_{LM}(\boldsymbol{R})f_{NL}\left(\frac{\sqrt{2}R}{l_0}\right) \tag{5}$$

where $Y_{LM}(\boldsymbol{R})$ are spherical harmonics and the numbers N and L run independently from zero to infinity. The radial functions $f_{NL}(\rho)$ are defined by†

$$f_{NL}(\rho)=K_{NL}\rho^L\exp(-\rho^2/2)\sum_{q=0}^{N}c_{NL,2q}\rho^{2q} \tag{6}$$

where the coefficients $c_{NL,2q}$ follow the recursion relation

$$c_{NL,0}=1 \qquad c_{NL,2q}=\frac{(q-N-1)}{q(q+L+1/2)}c_{NL,2q-2}. \tag{7}$$

The coefficients $c_{NL,2q}$ thus define an even polynomial that contains $(N+1)$ terms. The factor K_{NL} ensures that the functions $f_{NL}(\rho)$ are normalized

$$K_{NL}=\left[\sum_{q',q=0}^{N}c_{NL,2q'}c_{NL,2q}\frac{1}{2}\Gamma\left(L+q+q'+\frac{3}{2}\right)\right]^{-1/2}. \tag{8}$$

For the relative motion, equation (3) does not possess a simple analytical solution. We thus proceed to the diagonalization of the Hamiltonian in reduced Hilbert space. The eigenfunctions of the problem without Coulomb interaction are used as basis functions. In the absence of Coulomb interaction, equation (3) reduces to the problem of a three-dimensional harmonic oscillator with a particle of mass $m^*/2$. The corresponding eigenstates are labelled with a superscript '0'. The eigenenergies are

$$E_{\nu l}^0=\left(2\nu+l+\frac{3}{2}\right)\hbar\omega \tag{9}$$

† The radial functions $f_{NL}(r)$ can be expressed in terms of the confluent hypergeometric function ${}_1F_1$ (see [8]). We use the explicit development of the series in the text since it leads to an expression that can easily be implemented numerically for the matrix elements that follow in equation (11).

and the eigenfunctions are

$$\phi^0_{\nu lm}(\boldsymbol{r}) = \frac{1}{2^{3/4} l_0^{3/2}} Y_{lm}(\boldsymbol{r}) f_{\nu l}\left(\frac{r}{\sqrt{2} l_0}\right) \tag{10}$$

where ν and l run independently from zero to infinity. Using these functions as basis functions, we evaluate the matrix elements of the relative-motion Hamiltonian H^{rel} including Coulomb interaction, as defined by equation (3). These matrix elements are diagonal in all indices except ν

$$H^{rel}_{\nu' lm;\nu lm} = \delta_{\nu'\nu} E^0_{\nu lm} + \frac{l_0 \hbar\omega}{2\sqrt{2} a_0^*} K_{\nu' l} K_{\nu l} \sum_{q'=0}^{\nu'} \sum_{q=0}^{\nu} c_{\nu' l, 2q'} c_{\nu l, 2q} \Gamma(l + 1 + q + q'). \tag{11}$$

The diagonalization of H^{rel} is thus a very easy task. The matrix elements are readily evaluated and only a few basis functions are needed to obtain very good precision, as we will see in the next section. With $(\nu_{max}+1)$ basis functions, the result of the diagonalization gives the eigenenergies E_{nl} and their related coefficients d^n_ν, the integer index n running from zero to ν_{max}. The eigenfunctions of the relative motion are then given by

$$\phi_{nlm}(\boldsymbol{r}) = \sum_{\nu=0}^{\nu_{max}} d^n_\nu \phi^0_{\nu lm}(\boldsymbol{r}). \tag{12}$$

By combining the results, the eigenstates of the total Hamiltonian defined by equation (1) are characterized by the energies

$$E_{NL,nl} = E_{NL} + E_{nl} \tag{13}$$

and the wavefunctions:

$$\begin{aligned} \Psi_{NLM,nlm}(\boldsymbol{r}_1, \boldsymbol{r}_2) &= \Phi_{NLM}(\boldsymbol{R}) \phi_{nlm}(\boldsymbol{r}) \\ &= \frac{1}{l_0^3} Y_{LM}(\boldsymbol{R}) f_{NL}\left(\frac{\sqrt{2}R}{l_0}\right) Y_{lm}(\boldsymbol{r}) \sum_{\nu=0}^{\nu_{max}} d^n_\nu f_{\nu l}\left(\frac{r}{\sqrt{2} l_0}\right). \end{aligned} \tag{14}$$

We have yet to consider the spin. For such a two-particle problem, it can easily be introduced. The spatial properties related to the exchange of the two-particles are only governed by the relative-motion eigenfunction. It is symmetric (antisymmetric) for even (odd) values of l. The antisymmetrization of the total wavefunction including spin is then readily obtained by multiplying the wavefunction by a singlet (triplet) spin state for even (odd) values of l.

3. Results and discussion

Since the eigenenergies are independent of the magnetic numbers m and M, the various levels are identified by the simplified notation $|NL, nl\rangle$ where $N = 0, 1, 2, \ldots$ and $L =$ S, P, D, ... characterize the centre-of-mass motion while $n = 0, 1, 2, \ldots$ and $l =$ s, p, d, ... characterize the relative motion. Note that, in order to avoid the introduction of additional definitions, we do not use the so-called 'principal quantum numbers' [11] $(2L + 1)$ and $(2l+1)$ to identify the levels. The total degeneracy of the levels is given by $(2L+1)(2l+1)\theta_l$ where θ_l represents the spin degeneracy and takes a value of one for even values of l and a value of three for odd values of l.

Figure 1 presents the relative-motion energy E_{nl} as a function of the ratio l_0/a_0^*. This ratio gives an estimate of the relative strengths of the parabolic and Coulomb potentials. When $l_0 \ll a_0^*$, it is the strong confinement regime where the Coulomb repulsion can

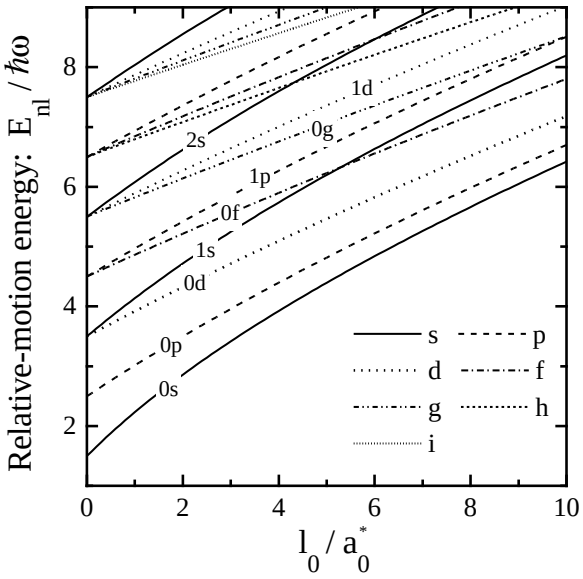

Figure 1. Relative-motion energy levels (E_{nl}) as a function of the ratio l_0/a_0^*. The various linetypes identify the levels according to the orbital quantum numbers of the relative-motion wavefunctions. The quantum numbers n and l are indicated for the lowest levels. As an illustration, for GaAs, $a_0^* \approx 105$ Å and the characteristic energy of the parabolic potential is $\hbar\omega \approx 0.1$ meV for $l_0/a_0^* = 10$ and $\hbar\omega \approx 10$ meV for $l_0/a_0^* = 1$.

be considered as a perturbation. When $l_0 \gg a_0^*$, the parabolic potential still ensures the confinement of the two electrons although the Coulomb repulsion contributes the most to the energy. The various linetypes identify the orbital quantum numbers of the relative-motion wavefunctions of the various levels. The lowest levels are also identified by their quantum numbers n and l. Each evaluation has been performed with eight basis functions. This ensures a precision† better than 0.2% in the worst case (the worst case being the 3s level near $l_0/a_0^* = 3.0$). In most cases, such a precision can be obtained with a smaller number of basis functions. For the 0s level, six basis functions give a precision better than 0.1% over the range of l_0/a_0^* values considered, while only three basis functions are necessary for a precision of 1%. For the 0p level, a 0.1% precision requires three basis functions while two basis functions ensure a 1% precision. We thus see that a good precision can be obtained with a very small computational effort.

Only the s-state wavefunctions do not vanish at the origin. Consequently, the related levels are the most sensitive to the Coulomb interaction. Since the states of various symmetries are differently affected by the Coulomb interaction, there are a lot of level crossings. The first level crossing appears between the singlet 1s level and the triplet 0f level near $l_0/a_0^* = 5.3$ at $E_{nl} = 6.3\hbar\omega$. It is interesting to point out that all the levels characterized by a given n value become quasi-degenerate at very high values of l_0/a_0^*. This only becomes evident for l_0/a_0^* much larger than ten (not shown on figure 1), but it can already be felt at $l_0/a_0^* = 10$ by noting that the four lowest levels are characterized

† The precision of an energy eigenvalue is estimated by comparing it to a reference value obtained in the following way. For a given level, the energies evaluated with different numbers (N) of basis functions (up to 32 functions in our work) are plotted as a function of $1/N$. The reference value is then taken as the asymptotic value when $1/N$ tends to zero.

by $n = 0$. This behaviour is a consequence of the accidental degeneracy related to the dynamical symmetry of the repulsive Coulomb potential. In fact, the level crossings occur due to the fact that we go from the accidental degeneracy of the harmonic potential at small l_0/a_0^* values to that of the repulsive Coulomb potential at large l_0/a_0^* values.

Figure 2 presents the total energy $E_{NL,nl}$ as a function of the ratio l_0/a_0^*. The numbers on the lowest levels indicate the total degeneracy. The various linetypes identify the levels that correspond to a given centre-of-mass motion energy (E_{NL}). The various center-of-mass states that have the same energy are identified by their N and L values on the legend. With the help of the curves provided in figure 1, one can easily identify the exact nature of the various levels of figure 2. All the curves corresponding to a given linetype (i.e. a given centre-of-mass energy) in figure 2 reproduce the curves of figure 1, up to a constant energy value. The lowest level of a given linetype in figure 2 thus corresponds to a relative-motion 0s state, the second lowest to a relative-motion 0p state, and so on. For example, the first band crossing that occurs at $E_{NL,nl} = 7.25\hbar\omega$ near $l_0/a_0^* = 5.8$ involves the $|0\mathrm{P}, 0\mathrm{s}\rangle$ and $|0\mathrm{S}, 0\mathrm{d}\rangle$ levels and is thus a singlet–singlet crossing.

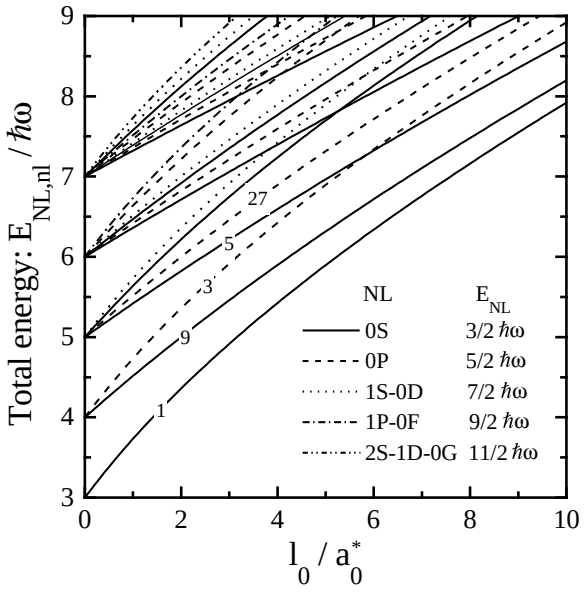

Figure 2. Energy levels ($E_{NL,nl}$) as a function of the ratio l_0/a_0^*. The various linetypes identify the levels corresponding to a given centre-of-mass energy (E_{NL}). The total degeneracy (product of the centre-of-mass, relative-motion and spin degeneracies) of the lowest levels is indicated by the numbers.

The curves in figure 2 can be compared with those provided by Zhu *et al* in figure 2 of [9]. The latter figure presents results for l_0/a_0^* varying from 0 to 5.6†. We obtain the same energies except for the lowest level ($|0\mathrm{S}, 0\mathrm{s}\rangle$) when $l_0/a_0^* > 3.0$, the difference being about 3% at $l_0/a_0^* = 5.6$, and for the $|0\mathrm{S}, 0\mathrm{g}\rangle$ level, our curve lying a little lower. The energy difference of the lowest level may be due to some fortuitous error in figure 2 of [9]. The variation of the energy for all the levels of the type $|NL, 0\mathrm{s}\rangle$ should be similar up

† The relation between the parameter γ defined in [6] and our notation is: $l_0/a_0^* = \sqrt{2/\gamma}$.

to an additional constant term ($E_{NL,0s} = (2N + L + 3/2)\hbar\omega + E_{0s}$). It is the case in our figure 2 and for all but the lowest level in the figure presented by Zhu *et al*. Note that the levels $|0S, 1p\rangle$, $|0P, 0f\rangle$, $|1S, 0p\rangle$ and $|0D, 0p\rangle$ (the latter two being degenerate) are missing in figure 2 of [9].

It is well known that, for a parabolic potential, the many-body effects due to Coulomb interaction are not directly accessible to far-infrared (FIR) spectroscopy [12, 13]. This can easily be seen here: a dipolar transition between relative-motion eigenstates is not allowed since a change $\Delta l = +/-1$ also implies a change of the spin state. It is interesting to note that interband spectroscopy has recently been used to highlight electron–electron interactions by looking at excitonic transitions in InAs self-assembled quantum dots [14].

Unlike the method of [9], our method provides for the wavefunction, a single expression that is valid over all space. It is interesting to see to what extent the Coulomb repulsion affects the electron relative motion. Figure 3 presents the radial part of the relative-motion wavefunction for the lowest level (0s), this wavefunction being quite sensitive to Coulomb interaction. One can appreciate that, as the electron confinement decreases (l_0/a_0^* increases), Coulomb interaction becomes more effective in determining the shape of the wavefunction by forcing the electrons to repel each other. To obtain a given precision on the wavefunctions, one needs more basis functions than for the evaluation of the eigenenergies. This is especially true for the short-range part of the relative-motion wavefunction, as already noted by Pfannkuche *et al* for a two-dimensional parabolic potential [8]. For example, eight basis functions ensure at least a precision of the order of 1% on the value of the 0s wavefunction for $r > l_0$ and for all values of l_0/a_0^*. On the other hand, the error on the value of the wavefunction at the origin exceeds 10% for $l_0/a_0^* > 2$. At $l_0/a_0^* = 5$, this difference can be brought down to less than 1% with 17 basis functions. The wavefunctions on figure 3 have been evaluated with 32 basis functions and can thus be considered exact results.

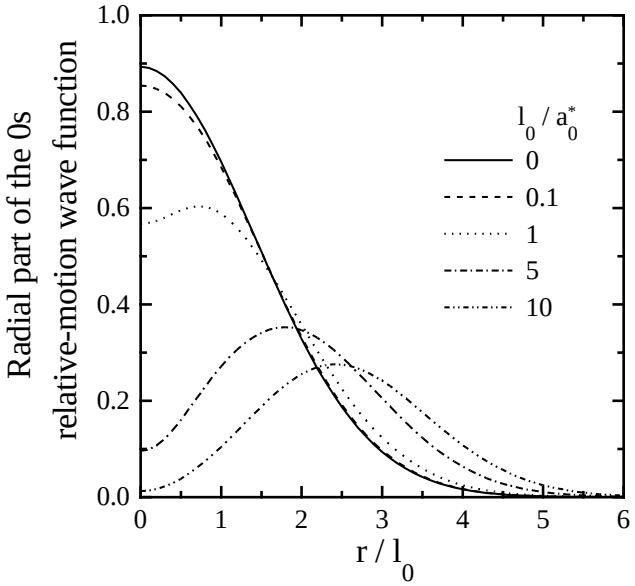

Figure 3. Radial part of the wavefunction for the lowest level (0s) of the relative motion for various values of the ratio l_0/a_0^*.

To get a broader picture of the effect of the Coulomb interaction on the wavefunctions, we plot in figure 4 the mean separation between the electrons (first moment of the radial part of the relative-motion wavefunction) as a function of l_0/a_0^* for the various levels. The linetypes again identify the curves according to the orbital quantum numbers of the relative motion. We see that the variation of the mean separation decreases as l and as n increase. For the range of l_0/a_0^* values considered, the separation almost doubles for the 0s level while the increase is less than 20% for the 1d level.

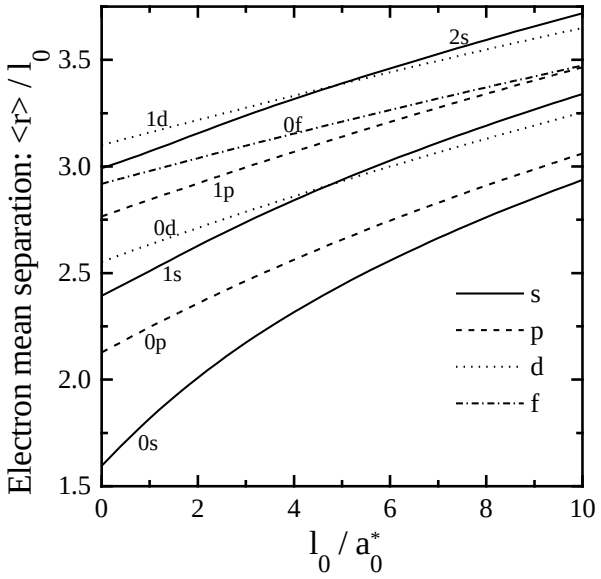

Figure 4. Mean separation between the electrons (first moment of the radial part of the relative-motion wavefunction) as a function of l_0/a_0^* for the lowest levels. The various linetypes identify the orbital quantum numbers of the relative motion.

We now consider two approximation methods for evaluating the level energies. In the first one, the Coulomb repulsion is considered as a perturbation that is evaluated to first order. The relative-motion approximate eigenenergies then correspond to the diagonal elements of the matrix defined in equation (11). This approximation is also considered in [9] although no direct comparison with more exact results are provided. We perform such a comparison further below.

To obtain the second approximation method, we note that the Coulomb interaction can be written as

$$\frac{e^2}{4\pi\epsilon r} = \frac{e^2\eta l_0}{4\pi\epsilon r^2} + \frac{e^2(r-\eta l_0)}{4\pi\epsilon r^2} \tag{15}$$

where η is a dimensionless parameter. By dropping the second term on the right-hand side, one obtains a $1/r^2$ potential that should provide a good approximation if the radial part of the relative-motion wavefunction is well concentrated around ηl_0. This approximate potential is of interest since it leads to an analytical solution, as sketched in the appendix, with the relative-motion energy levels

$$E_{nl} = \left(2n + 1/2\sqrt{1 + 4[l(l+1) + \eta l_0/a_0^*]} + 1\right)\hbar\omega. \tag{16}$$

In our calculations, we have arbitrarily opted for the simplest choice for the parameter η. For a given relative-motion state characterized by the quantum numbers (n, l, m), we have used the mean distance between the two electrons $(\langle r \rangle / l_0)$ evaluated with the function $\phi^0_{nlm}(\boldsymbol{r})$ (equation (10)) to which the eigenstate reduces in absence of Coulomb repulsion.

Figure 5 shows the relative-motion energy levels evaluated with the two approximation methods along with the more exact results obtained by diagonalizing H^{rel} (equation (11)) with eight basis functions.

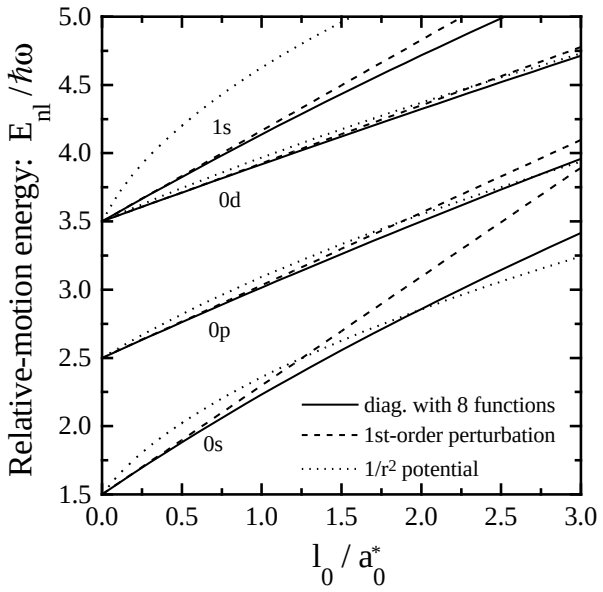

Figure 5. Relative-motion energy levels (E_{nl}) as a function of the ratio l_0/a^*_0 as evaluated with the first-order perturbation calculation (dashed curves) and with the approximate $1/r^2$ potential (dotted curves). They are compared with the more exact results obtained from the diagonalization of the relative-motion Hamiltonian with eight basis functions (full curves).

The precision of the first-order perturbation calculation increases with l and n. This is a simple consequence of the fact that the true wavefunction is less affected by the Coulomb repulsion as l and n increase, as indicated by figure 4, so the zeroth order wavefunction remains a good approximation over a wide range of l_0/a^*_0 values. For the ground state (0s), this approximation provides a precision better than 10% on the energy difference $(E_{0s} - 1.5)\hbar\omega$ up to $l_0/a^*_0 \approx 1.1$. For the 1s and 0p levels, a similar precision is obtained up to $l_0/a^*_0 \approx 2.1$ and $l_0/a^*_0 \approx 3.2$, respectively.

The $1/r^2$ potential gives acceptable results only for the $n = 0$ states. This is due to the fact that the validity of the $1/r^2$ potential is expected to increase with the localization of the relative-motion wavefunction and only the $n = 0$ states have a 'one-lobe' radial function that is somewhat localized. Note that for the 0s level, the wavefunction lies very close to the origin, so this potential still does not provide a very good approximation since $1/r^2$ varies rapidly.

4. Conclusion

We have presented a simple solution to the problem of two interacting electrons confined by a three-dimensional parabolic quantum dot. The method is based on the diagonalization of the relative-motion Hamiltonian in reduced Hilbert space. This diagonalization is easily performed since the matrix elements are evaluated analytically and only a few basis functions are needed to obtain a good precision on the energy levels.

The results agree with those previously published by Zhu *et al* [9]. However, our method is more straightforward and easier to implement numerically. Furthermore, unlike the method of [5], our approach gives a single expression that is valid over all space for the wavefunction.

Two approximation schemes have been considered. The first-order perturbation approach has been seen to be quite useful for estimating the level energies. The approximate $1/r^2$ potential with $\eta = \langle r \rangle / l_0$ has been seen to provide a decent approximation only for the $n = 0$ relative-motion states.

Acknowledgments

This work has been supported by the Laboratoire d'Electronique de Technologie et d'Instrumentation (LETI, Grenoble, France). One of us (GL) also wants to thank the Conseil National de Recherches en Sciences Naturelles et en Génie (CRSNG) du Canada for financial support in the form of a postdoctoral fellowship.

Appendix

In this appendix, we sketch the evaluation of the energy levels of the approximate $1/r^2$ interaction potential. In that case, the relative-motion Schrödinger equation (equation (3)) becomes

$$\left[-\frac{\hbar^2}{2(m^*/2)}\nabla_r^2 + \frac{1}{2}\left(\frac{m^*}{2}\right)\omega^2 r^2 + \frac{e^2\eta l_0}{4\pi\epsilon r^2}\right]\phi_{nlm}(\boldsymbol{r}) = E_{nl}\phi_{nlm}(\boldsymbol{r}). \tag{A1}$$

We introduce $\boldsymbol{\rho} = \boldsymbol{r}/(\sqrt{2}l_0)$ and we look for a solution of the form

$$\phi_{nlm}(\boldsymbol{\rho}) = \frac{Y_{lm}(\boldsymbol{\rho})u_{nl}(\rho)}{\rho}. \tag{A2}$$

The radial equation satisfied by $u_{nl}(\rho)$ can be written in the following form

$$\left[-\frac{\mathrm{d}^2}{\mathrm{d}\rho^2} + \frac{\alpha(\alpha+1)}{\rho^2} + \rho^2 - \frac{2E_{nl}}{\hbar\omega}\right]u_{nl}(\rho) = 0 \tag{A3}$$

where

$$\alpha = -1/2 + 1/2\sqrt{1 + 4[l(l+1) + \eta l_0/a_0^*]}. \tag{A4}$$

Equation (A3) is identical to the radial equation obtained in the problem of an harmonic oscillator if we replace α by the orbital quantum number l. The eigenenergies for the harmonic oscillator problem have already been expressed in terms of l in equations (4) and (9). Replacing l by α, one readily obtains the eigenenergies of the $1/r^2$ interaction potential as given by equation (16).

References

[1] Johnson N F 1995 *J. Phys.: Condens. Matter* **7** 965
[2] Hanafi H, Tiwari S and Khan I 1996 *IEEE Trans. Electron Devices* **43** 1553
[3] Welser J J, Tiwari S, Rishton S, Lee K Y and Lee Y 1997 *IEEE Electron. Device Lett.* **18** 278
[4] Guo L, Leobandung E and Chou S 1997 *Science* **275** 649
[5] Ashoori R C, Stormer H L, Weiner J S, Pfeiffer L N, Baldwin K W and West K W 1993 *Phys. Rev. Lett.* **71** 613
[6] Meurer B, Heitmann D and Ploog K 1992 *Phys. Rev. Lett.* **68** 1371
[7] Su B, Goldmann V J and Cunningham J E 1992 *Phys. Rev.* B **46** 7644
[8] Pfannkuche D, Gudmundsson V and Maksym P A 1993 *Phys. Rev.* B **47** 2244
[9] Zhu J L, Li Z Q, Yu J Z, Ohno K and Kawazoe Y 1997 *Phys. Rev.* B **55** 15 819
[10] Stehle P 1966 *Quantum Mechanics* (San Francisco, CA: Holden-Day) p 82
[11] Greiner W 1989 *Quantum Mechanics: An Introduction* 2nd edn (Berlin: Springer) p 126
[12] Maksym P A and Chakraborty T 1990 *Phys. Rev. Lett.* **65** 108
[13] Peeters F M 1990 *Phys. Rev.* B **42** 1486
[14] Warburton R J, Dürr C S, Karrai K, Kotthaus J P, Medeiros-Ribeiro G and Petroff P M 1997 *Phys. Rev. Lett.* **79** 5282